

Plasma energy and work function of conducting transition metal nitrides for electronic applications

G. M. Matenoglou, L. E. Koutsokeras, and P. Patsalas

Citation: *Appl. Phys. Lett.* **94**, 152108 (2009); doi: 10.1063/1.3119694

View online: <http://dx.doi.org/10.1063/1.3119694>

View Table of Contents: <http://apl.aip.org/resource/1/APPLAB/v94/i15>

Published by the [American Institute of Physics](#).

Additional information on Appl. Phys. Lett.

Journal Homepage: <http://apl.aip.org/>

Journal Information: http://apl.aip.org/about/about_the_journal

Top downloads: http://apl.aip.org/features/most_downloaded

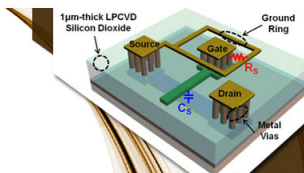
Information for Authors: <http://apl.aip.org/authors>

ADVERTISEMENT



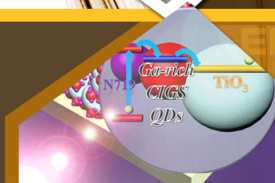
**EXPLORE WHAT'S
NEW IN APL**

SUBMIT YOUR PAPER NOW!



SURFACES AND INTERFACES

Focusing on physical, chemical, biological, structural, optical, magnetic and electrical properties of surfaces and interfaces, and more...



ENERGY CONVERSION AND STORAGE

Focusing on all aspects of static and dynamic energy conversion, energy storage, photovoltaics, solar fuels, batteries, capacitors, thermoelectrics, and more...

Plasma energy and work function of conducting transition metal nitrides for electronic applications

G. M. Matenoglou, L. E. Koutsokeras, and P. Patsalas^{a)}

Department of Materials Science and Engineering, University of Ioannina, Ioannina, 45110, Greece

(Received 9 February 2009; accepted 24 March 2009; published online 16 April 2009)

The combination of electrical conductivity, chemical and metallurgical stability, refractory character, having lattice constants that are close to those of III-nitrides makes transition metal nitrides promising candidates for electronics and device applications. We study the structure, stability, and the plasma energy of stoichiometric, transition metal nitrides of similar crystal quality as well as the widest variety of their ternaries ever reported. We establish the phase spaces of the plasma energy (6.9–10.5 eV) and the work function (3.7–5.1 eV) of these complex nitrides with their lattice constant (0.416–0.469 nm) and we investigate the limits of their applications. © 2009 American Institute of Physics. [DOI: 10.1063/1.3119694]

The nitrides of group IVb–VIb transition metals (TMNs) exhibit a unique combination of electron conductivity, refractory character, high hardness, chemical inertness, and a cubic rocksalt structure with a lattice constant close to those of III-nitrides. These properties make them suitable for applications in electronics, such as diffusion barriers,^{1–3} metallizations,^{4–6} and growth templates for wide bandgap semiconductors^{4–6} and as components in microelectromechanical systems (MEMS).^{7,8} It is critical, however, that TMN's electronic properties should be combined with the lattice constant matching to the substrate's lattice in order to prevent device's degradation and failure due to the formation of misfit dislocations.⁵ Therefore, conducting ternary nitrides with tailored lattice constant can be very promising candidates replacing the currently used TiN and TaN. Such ternary compounds have been reported^{9–15} but still their electronic properties have yet not been investigated with respect to their lattice constant. In this work we present a thorough study of the crystal structure, the work function (WF) and the plasma energy E_p for the widest range of binary TMN and ternary $\text{Ti}_x\text{Me}_{1-x}\text{N}$ and $\text{Ta}_x\text{Me}_{1-x}\text{N}$ (Me=Ti, Zr, Hf, Nb, Ta, Mo, W) films reported ever.

All the films have been grown by pulsed laser deposition¹³ and exhibit a $[\text{Me}]/[\text{N}]$ ratio very close to unity ($\leq \pm 2\%$). Ternary films of varying x were investigated using *in situ* Auger electron spectroscopy analysis. X-ray diffraction (XRD) patterns, acquired in θ - 2θ geometry, exhibit just the (111) and (200) peaks of the rocksalt structure (Fig. 1), without any fine structure, indicating perfect solid solutions over the full range of x ($0 < x < 1$). The lattice constants (α) are calculated from the (111) XRD peak and are displayed in Fig. 2, where they are compared with the reference values from the powder data for the binary nitrides,¹⁶ as well as with the values anticipated when Vegard's rule applies for the ternary systems. The α versus x curves for three sets of films ($\text{Ti}_x\text{Zr}_{1-x}\text{N}$, $\text{Ti}_x\text{Ta}_{1-x}\text{N}$, and $\text{W}_x\text{Ta}_{1-x}\text{N}$) are presented (Fig. 2, inset) and follow distinct straight lines resembling Vegard's rule. In all cases, α is expanded compared to the expected values; this is solely due to in-plane compressive stresses, which are associated with the growth and are re-

lieved after vacuum annealing (Fig. 2, blue stars).¹³

Correlating the α with the film composition for the systems $\text{Ti}_x\text{Zr}_{1-x}\text{N}$ (IVb–IVb–N), $\text{Ti}_x\text{Ta}_{1-x}\text{N}$ (IVb–Vb–N) and $\text{W}_x\text{Ta}_{1-x}\text{N}$ (Vb–VIb–N) demonstrates the global validity of Vegard's rule, independently of the valence electron configuration of the two constituent metals. The ability of tailoring the lattice constant of conducting nitrides over the vast range of 0.416–0.469 nm makes these complex nitrides promising as conducting epilayers onto various sublayers achieving very low lattice mismatch.

The optical properties were studied using optical reflectance spectroscopy (ORS) (Fig. 3, inset), which revealed the typical behavior of conductors. Thus, the optical data were analyzed to the contributions of intraband and interband transitions described by a Drude term and two Lorentz oscillators, respectively.¹⁷ This modeling determines accurately the plasma energy E_p , which is directly correlated with the conduction electron density N ,

$$E_p = \hbar \omega_p, \omega_p = \sqrt{\frac{Ne^2}{\epsilon_0 m^*}}, \quad (1)$$

(where e is the electron charge, ϵ_0 is the permittivity of free space, and m^* is the electron effective mass, in SI units). E_p

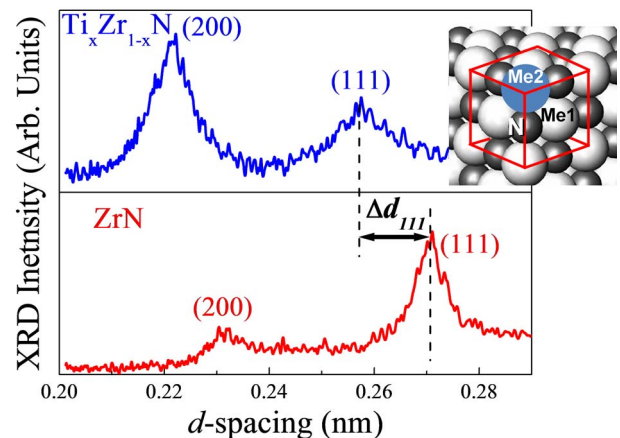


FIG. 1. (Color online) XRD patterns from ZrN and $\text{Ti}_x\text{Zr}_{1-x}\text{N}$ films revealing their rocksalt structure with the one metal being in substitutional positions of the other (inset).

^{a)}Author to whom correspondence should be addressed. Electronic mail: ppats@cc.uoi.gr.

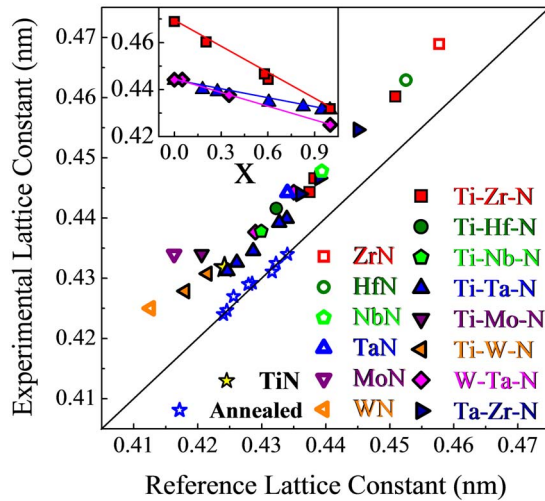


FIG. 2. (Color online) Comparison of the experimental lattice constants with those expected from Vegard's rule. Inset: Correlations of the lattice constant with the film composition for the systems $\text{Ti}_x\text{Zr}_{1-x}\text{N}$, $\text{Ti}_x\text{Ta}_{1-x}\text{N}$, and $\text{W}_x\text{Ta}_{1-x}\text{N}$.

is an intrinsic property of the material because it determines the electron conductivity at zero temperature and with zero defects.¹⁷ Of course for realistic device applications the electron scattering, which is affected by the structural defects and the temperature, is also very important and should be taken into account.¹⁷ The following correction: $(E_p^{\text{cor}}/E_p)^2 = \rho_{\text{ref}}/\rho_{\text{exp}}$, where ρ_{ref} and ρ_{exp} are the reference and experimental mass density measured by x-ray reflectivity for each case, respectively, has been applied in order to deduce the E_p values of the fully dense films presented in Fig. 3.

E_p^2 values are rationally grouped according to the metal's quantum numbers (principal quantum number and number of valence electrons), as shown in Fig. 3. Nitrides of metals of the same group (e.g., TiN, ZrN, and HfN, whose metals share the same d^2s^2 valence electron configuration) exhibit similar E_p^2 values, while E_p^2 increases with increasing number of valence electrons. This is quite reasonable if we take into account that part of the metal's valence charges are hybridized to form the covalent bonding with N and the excess of the metal's electrons (which are increasing with increasing

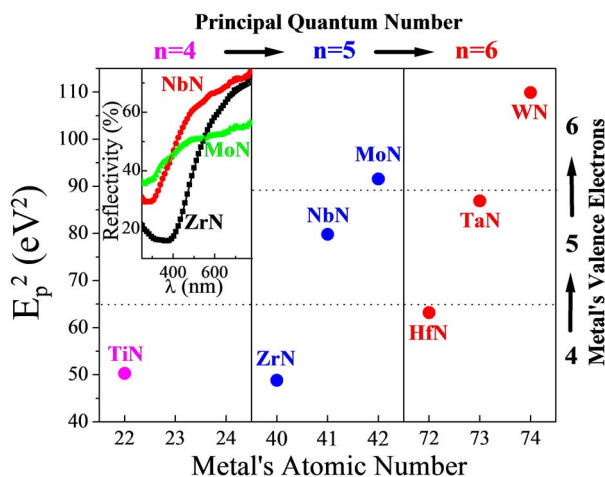


FIG. 3. (Color online) The variation of E_p^2 for binary TMN, which are grouped according to the number of valence electrons of the constituent metal. Inset: ORS experimental and fitted spectra of row-5 TMN.

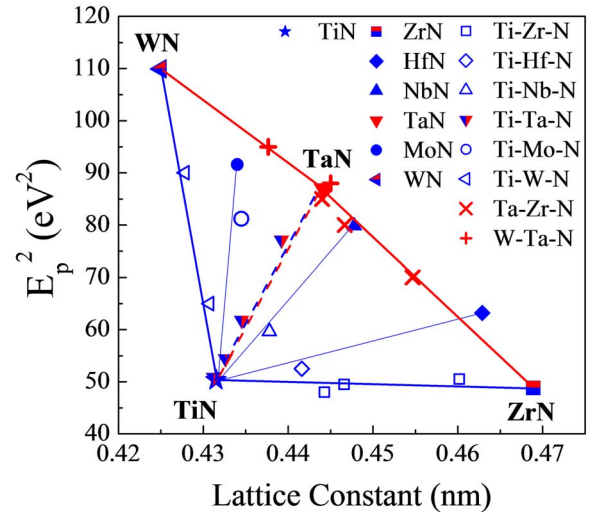


FIG. 4. (Color online) The phase space of E_p^2 (which is proportional to conduction electron density) vs. the nitride's lattice constant.

number of metal's valence electrons) constitute the Fermi gas.

The E_p^2 values of each ternary nitride system follow an almost linear correlation with the α , as shown in Fig. 4, and the composition x of the films. The more generalized view of E_p^2 versus α for all the binary and ternary nitrides is much more complex. Thus, the phase space of E_p^2 with the nitride's α has an almost triangular shape with TiN, ZrN, and WN being at the vertices; TaN is also indicated in Fig. 4 for comparison. The form of this phase space reveals that $\text{Ti}_x\text{Zr}_{1-x}\text{N}$ is the most versatile system for low-mismatch growth on various semiconductors since it exhibits almost constant E_p^2 (i.e., conduction electron density) and varying α in the vast range of 0.432–0.469 nm. On the other hand, the $\text{Ti}_x\text{W}_{1-x}\text{N}$ system provides the ability to grow conducting epilayers of similar α (below 0.430 nm) but with E_p^2 considerably varying; as a result, conducting layers of varying resistivity can be grown, e.g., for MEMS applications. The whole phase space can be covered by alloying the various nitrides.

Another important factor for Ohmic behavior of a contact is the WF of the conductor. In the case of n -type semiconductors, the metal's WF should be equal to the electron affinity of the semiconductor.¹⁸ Relative WF values of selected $\text{Ti}_x\text{Zr}_{1-x}\text{N}$ samples have been determined by *ex situ* Kelvin probe measurements. In order to estimate the absolute values, these relative values were scaled to the value $\text{WF}_{\text{TiN}} = 3.74$ eV of a reference, stoichiometric TiN sample (assuming that possible adsorbates from the ambient would be the same for all samples), and are presented in Fig. 5 along with the values of various binary nitrides reported in Refs. 19 and 20 (for comparison), and the electron affinities and lattice constants of III-nitride semiconductors. We note here that for simplicity the lattice constants of III-nitrides presented in Fig. 5 are for the zincblende polytypes; in the case of the wurtzite polytypes, the picture is similar for heteroepitaxy of the (111) rocksalt conductor nitride along the (0001) III-nitride semiconductor.⁵ It is evident that $\text{Ti}_x\text{Zr}_{1-x}\text{N}$ is structurally and electrically appropriate as growth template or Ohmic contact for n -type $\text{In}_y\text{Ga}_{1-y}\text{N}$. Following similar considerations¹⁸ and taking into account the bandgap values

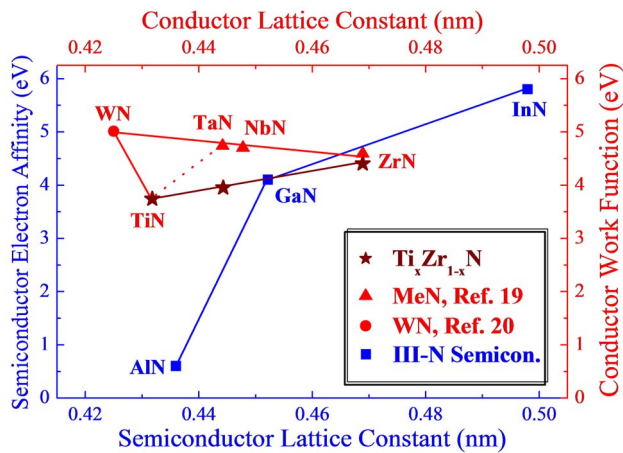


FIG. 5. (Color online) The variation of WF with the nitride's lattice constant in comparison with the electron affinities and the lattice constants of III-nitrides.

of the III-nitrides, $W_xTa_{1-x}N$ might be also promising as contact on p -type $Al_yGa_{1-y}N$.

In conclusion, conducting, ternary TMN are stable in the rocksalt structure independently of the valence electron configuration of the two constituent metals. They exhibit a vast range of lattice constants, plasma energies and WFs making them suitable for various electronic applications. Taking into account the valence electron configuration and the lattice constants of the constituent binary nitrides it is possible to grow nitride conductors of similar lattice constant and varying conduction electron density and vice versa. Especially for $Ti_xZr_{1-x}N$, the correlation of the lattice constant and WF is such as to constitute a promising metallization for $In_yGa_{1-y}N$.

We acknowledge Professor C. Kosmidis and the Central Laser Facility of the Univ. Ioannina for providing the laser, Dr S. Kassavetis (AUTH) for the Kelvin probe measurements, and Professor T. D. Moustakas (Boston University) and Dr. E. Lidorikis (University of Ioannina) for critical discussions.

- ¹A. E. Kaloyeros and E. Eisenbraun, *Annu. Rev. Mater. Sci.* **30**, 363 (2000).
- ²Y.-S. Wang, W.-H. Lee, Y.-L. Wang, C.-C. Hung, and S.-C. Chang, *J. Phys. Chem. Solids* **69**, 601 (2008).
- ³D. Adams, G. F. Malgas, N. D. Theodore, R. Gregory, H. C. Kim, E. Misra, T. L. Alford, and J. W. Mayer, *J. Vac. Sci. Technol. B* **22**, 2345 (2004).
- ⁴M. H. Oliver, J. L. Schroeder, D. A. Ewoldt, I. H. Wildeson, V. Rawat, R. Colby, P. R. Cantwell, E. A. Stach, and T. D. Sands, *Appl. Phys. Lett.* **93**, 023109 (2008).
- ⁵P. Ruterana, G. Nouet, Th. Kehagias, Ph. Komninou, Th. Karakostas, M. A. di Fort-Poisson, F. Huet, and H. Morkoc, *Phys. Status Solidi A* **176**, 767 (1999).
- ⁶T. Seppänen, L. Hultman, J. Birch, M. Beckers, and U. Kreissig, *J. Appl. Phys.* **101**, 043519 (2007).
- ⁷W. W. Jang, J. O. Lee, J.-B. Yoon, M.-S. Kim, J.-M. Lee, S.-M. Kim, K.-H. Cho, D.-W. Kim, D. Park, and W.-S. Lee, *Appl. Phys. Lett.* **92**, 103110 (2008).
- ⁸V. Cimalla, J. Pezoldt, and O. Ambacher, *J. Phys. D* **40**, 6386 (2007).
- ⁹A. Hoerling, J. Sjöln, H. Willmann, T. Larsson, M. Odén, and L. Hultman, *Thin Solid Films* **516**, 6421 (2008).
- ¹⁰G. Abadias and Ph. Guerin, *Appl. Phys. Lett.* **93**, 111908 (2008).
- ¹¹N. N. Iosad, N. M. van der Pers, S. Grachev, V. V. Roddatis, B. D. Jackson, S. N. Polyakov, P. N. Dmitriev, and T. M. Klapwijk, *J. Appl. Phys.* **92**, 4999 (2002).
- ¹²S. M. Aouadi, *J. Appl. Phys.* **99**, 053507 (2006).
- ¹³L. E. Koutsokeras, G. Abadias, Ch. E. Lekka, G. M. Matenoglou, D. F. Anagnostopoulos, G. A. Evangelakis, and P. Patsalas, *Appl. Phys. Lett.* **93**, 011904 (2008).
- ¹⁴T. Joelsson, L. Hultman, H. W. Hugosson, and J. M. Molina-Aldareguia, *Appl. Phys. Lett.* **86**, 131922 (2005).
- ¹⁵C.-S. Lee, E.-Y. Chang, L. Chang, C.-Y. Fang, Y.-L. Huang, and J.-S. Huang, *Jpn. J. Appl. Phys., Part 1* **42**, 4193 (2003).
- ¹⁶JCPDS Card No. 38-1420; JCPDS Card No. 81-1550; JCPDS Card No. 33-592; JCPDS Card No. 38-1155; JCPDS Card No. 49-1283; JCPDS Card No. 42-1120; JCPDS Card No. 25-1257.
- ¹⁷G. M. Matenoglou, L. E. Koutsokeras, Ch. E. Lekka, G. Abadias, S. Camelio, G. A. Evangelakis, C. Kosmidis, and P. Patsalas, *J. Appl. Phys.* **104**, 124907 (2008); P. Patsalas and S. Logothetidis, *ibid.* **90**, 4725 (2001); **93**, 989 (2003).
- ¹⁸S. M. Sze, *Physics of Semiconductor Devices*, 2nd ed. (Wiley, New York, 1981).
- ¹⁹Y. Gotoh, H. Tsuji, and J. Ishikawa, *J. Vac. Sci. Technol. B* **21**, 1607 (2003).
- ²⁰P.-C. Jiang, Y.-S. Lai, and J. S. Chen, *Appl. Phys. Lett.* **89**, 122107 (2006).